Induced Side Forces at High Angles of Attack

Andrew B. Wardlaw Jr.* and Alfred M. Morrison*
Naval Surface Weapons Center, White Oak Laboratory, Silver Spring, Md.

Linear regression techniques are used to establish a quantitative description of side forces on bodies of revolution at high incidence and zero side slip. A data base is assembled concerning the key side force characteristics of maximum measured side force, angle of attack at which it occurs, and minimum angle of incidence at which a side force is observed (onset angle). This information is examined to determine the important trends, and a linear regression model is developed for these quantities to include only those variables which are statistically significant. Results indicate that the peak side force coefficient is a function of Mach number, and only slightly of Reynolds number. Nose fineness is the critical model dimension which suggests that peak side forces are a product of the nose flowfield. Blunting of the nose reduces the magnitude of the side force but the degree of bluntness does not appear to be important. The angle at which the maximum side force occurs is found to be dependent on model length and Mach number, while the onset angle is a function of model length only.

Nomenclature

C_L = lift coefficient of cylinder in crossflow $= F_L/qD^2\ell_t$
C_Y = side force coefficient on a body at incidence $= F_y/q\frac{\pi D^2}{4}$
C_{ym} = absolute value of maximum observed C_Y
D = base diameter
$\bar{D}$ = average diameter $= \frac{1}{\ell_t D}\int_0^{\ell_t D} D\,dx$
ℓ_n = nose length/D
ℓ_t = model length/D
$\bar{\ell}_t$ = model length/$\bar{D}$
M = Mach number
M_c = crossflow Mach number $= M\sin\alpha$
q = freestream dynamic pressure
Re = Reynolds number based on diameter
Re_c = crossflow Reynolds number $- Re\sin\alpha$
r_b = nosetip radius/D
t = time
t^* = dimensionless time $= Ut/D$
U = freestream velocity
x = longitudinal distance along model measured from nosetip
α = angle of attack in degrees
α_0 = onset angle in degrees (minimum angle of attack at which a side force is observed)
α_m = angle of attack at which maximum side force is observed in degrees

Introduction

BODIES with pitch plane symmetry experience steady or quasisteady side loads at high angles of attack in subsonic and transonic flow. These forces generally occur between 0° to 60° incidence and can be traced to the formation of an asymmetric vortex pattern in the leeward flowfield. The magnitude of the side force has been observed to exceed that of the normal force on short bodies ($\ell_t \leq 4$).[1]

To date, side forces have been the subject of several studies[1-5] which have determined that the magnitude of these loads decreases with increasing Mach number, decreasing nose fineness, and the introduction of bluntness. No conclusions have been offered concerning the influence of Reynolds number, and the addition of grit has been observed to increase these forces in some cases and decrease them in others.

A quantitative description of side forces has not emerged. These loads are extremely sensitive to factors which are difficult to control, such as small irregularities in model geometry, and seemingly insignificant changes in test conditions and/or procedures. Rolling an axisymmetric model drastically alters the measured side force and the accompanying vortex pattern. Figure 1 shows changes in flowfield structure as seen on schlieren photographs, while Fig. 2 gives an example of variations in side force. This extreme sensitivity has been traced by some observers to irregularities in the model construction on the order of the machining tolerances;[6,7] however, the fact that side-force measurements taken at roll angles differing by 180° are not necessarily mirror images of one another (as in Fig. 2) indicates that other factors are important. A description of side forces is further compilcated by flowfield instabilities which have been observed to be interspersed with the steady asymmetric pattern.[7] Although the steady mode appears to be dominant, assumption of a completely steady flow pattern is an idealization of the situation.

A description of induced side force must be based on a large number of experimental measurements. Because of the sensitive nature of this load, conclusions founded on a small number of observations may be incorrect both qualitatively and quantitatively. An appropriate procedure for the analysis of side-force data is to develop a large data base and to apply linear regression methods to produce a quantitative description of it. To obtain meaningful results a careful analysis of the data base must be combined with an aerodynamic understanding of the problem. Linear regression techniques develop a least-squares fit description of a parameter, including those independent variables which are statistically significant. This procedure only provides criteria for determining whether a relation exists between two variables. It is up to the user to select pertinent variable groupings and their appropriate functional form.

In the current paper a quantitative description of key side-force characteristics is developed by applying linear regression techniques to a data base collected in available literature[1-5,8-12] and from private sources. Attention is focused on the key features of maximum observed side force, angle of attack at which it occurs, and the lowest angle of attack at which a side force is measured.

Of principal interest in this paper is the method of analysis rather than the specific results. In the near future data bases

Received Dec. 4, 1975; revision received April 28, 1976. Sponsored by the Naval Air Systems Command, AIR 320C.
Index categories: LV/M Aerodynamics; Nonsteady Aerodynamics.

*Aerospace Engineer, Experimental Aerodynamics Branch. Member AIAA.

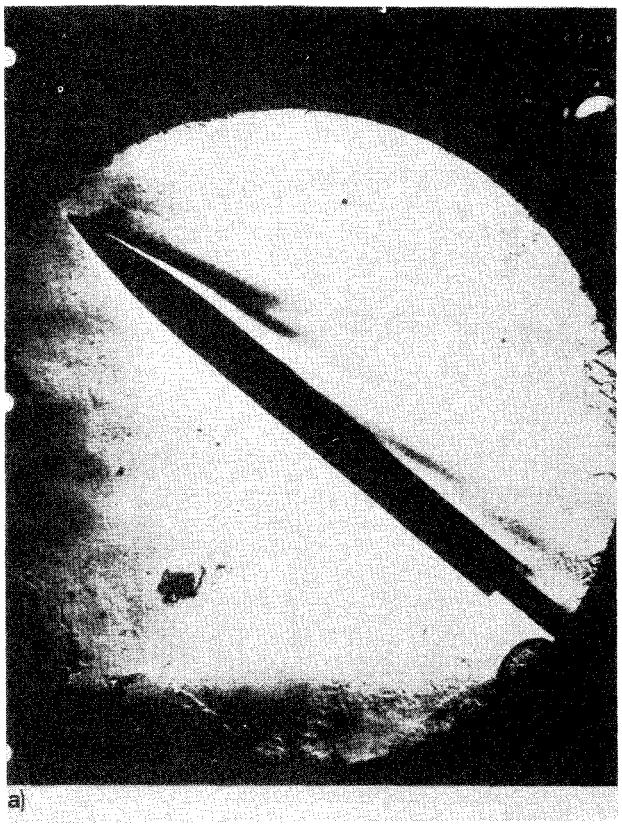

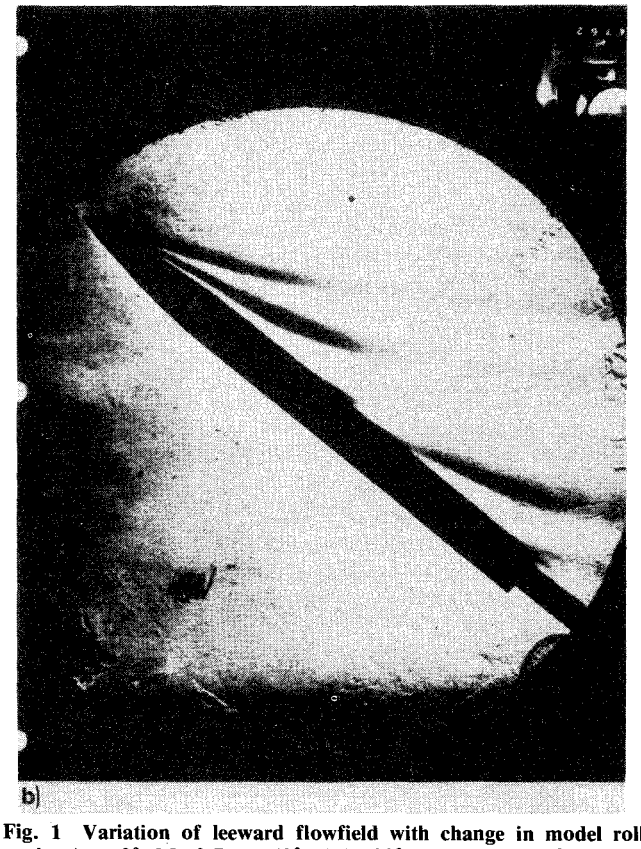

Fig. 1 Variation of leeward flowfield with change in model roll angle. a) $\phi = 0°$, $M = 0.7$, $\alpha = 40°$; b) $\phi = 90°$, $M = 0.7$, $\alpha = 40°$.

can be expected to expand, and thereby yield an improved understanding of the high angle-of-attack flowfield. These developments will make a more accurate description of side force possible. Also, data may become available which will allow the assessment of the effect of tunnel turbulence level, model machining tolerance, model surface finish and the

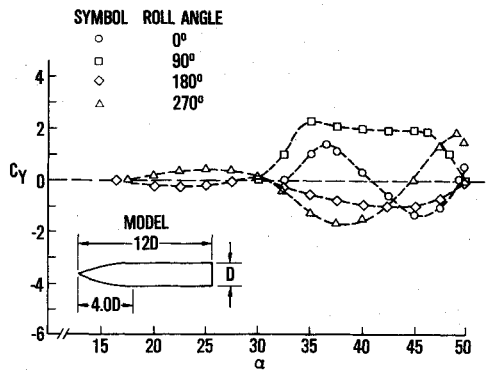

Fig. 2 C_y vs α at several different roll orientations. Data taken from Ref. 12 ($M = 0.9$).

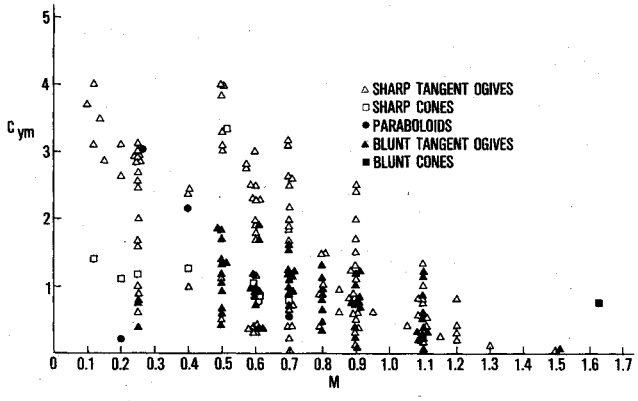

Fig. 3 C_{ym} vs M for all points in the data base.

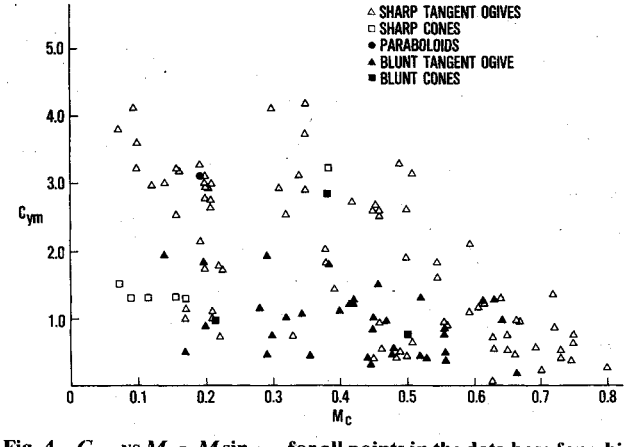

Fig. 4 C_{ym} vs $M_c = M \sin \alpha_m$ for all points in the data base for which α_m is known.

model mounting arrangement. Inclusion of these variables in a regression model will allow wind-tunnel results to be applied more accurately to the flight of production vehicles. For the present, the side force description developed in this article fulfills a unique need by providing a quantitative estimate of key side force characteristics.

Data Base

The data base, which is listed in Ref. 13, is comprised of a total of 208 cases. All cases are taken to be of equal validity. A value of C_{ym} is obtained for each case and, where possible, α_m and α_0 are also determined. In some instances these two quantities could not be read clearly, and in others information is taken from charts showing C_{ym} only. The variable α_m is recorded for 118 cases, and α_0 for 112. In situations where two side-force peaks of nearly equal magnitude occur, both

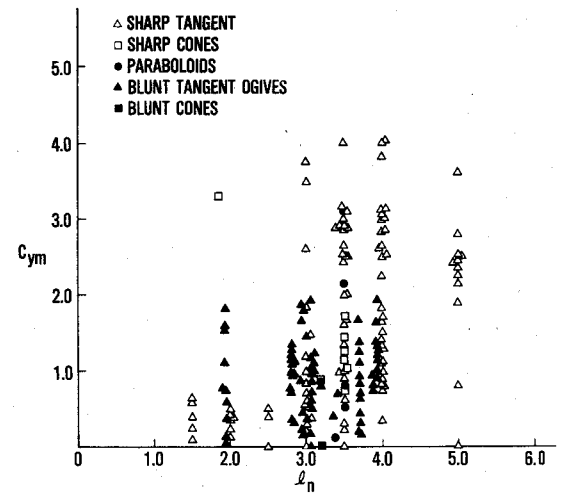

Fig. 5 C_{ym} vs ℓ_n for all points in the data.

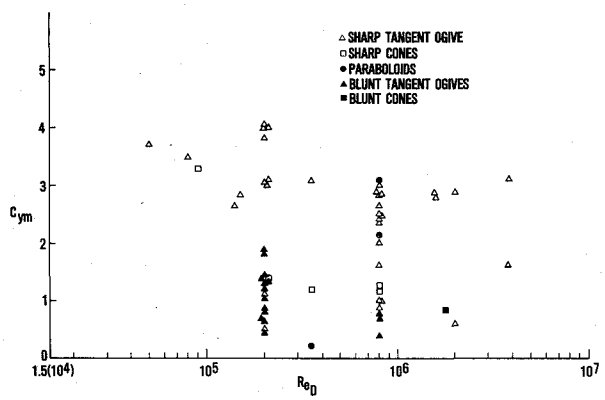

Fig. 6 C_{ym} vs Re for all data having $M<0.57$.

C_{ym} and α_m values are noted. The quantity α_0 is taken to be the largest value of α at which a zero side force is measured.

An examination of the data indicates that M or M_c is an important determinant of C_{ym}, particularly in the high subsonic regime where the crossflow Mach number is supercritical. The general trend is for decreasing values of side force with increasing M. The parameter C_{ym} is plotted as a function of M and M_c in Figs. 3 and 4, respectively. Smaller ℓ_n values also result in decreasing C_{ym}, as is illustrated in Fig. 5. An analysis of the data indicate that this trend is more pronounced at higher Mach numbers. The relation between Re and C_{ym}, which is explored in Fig. 6, does not indicate a strong dependency between these quantities.

The different side force characteristics of blunt and sharp tangent ogive bodies are clearly illustrated in Figs. 3-5. Dependencies are much more clearly defined for sharp bodies, particularly in the case of ℓ_n. The relation between C_{ym} and r_b on blunt bodies is shown in Fig. 7 and does not indicate a well-defined relation between these two variables. Thus, it appears that although bluntness is an important factor, the degree of bluntness is not significant.

The data of Fig. 3 show that side forces generally disappear for $M>1.4$, the only exception being a measurement taken on a cone. There is another example available which shows a small but measurable side force on a cone at $M=2.00$.[14] This suggests that cones experience side-force effects to a higher Mach number than tangent ogives. In Fig. 4 it is shown that for all classes of bodies, side force disappears at $M_c>0.8$. Thomson has found that vortices in the leeward flowfield start to lose their characteristic form at $M_c>0.7$.[7]

An examination of the data base indicates that α_m is related to $\bar{\ell}_t$ and M, while α_0 is principally a function of $\bar{\ell}_t$. Data for these three relations are presented in Figs. 8-10, respectively.

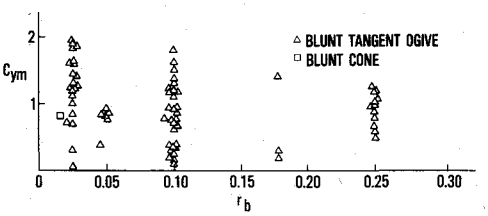

Fig. 7 C_{ym} vs r_b for all blunt models ($r_b>0.005$).

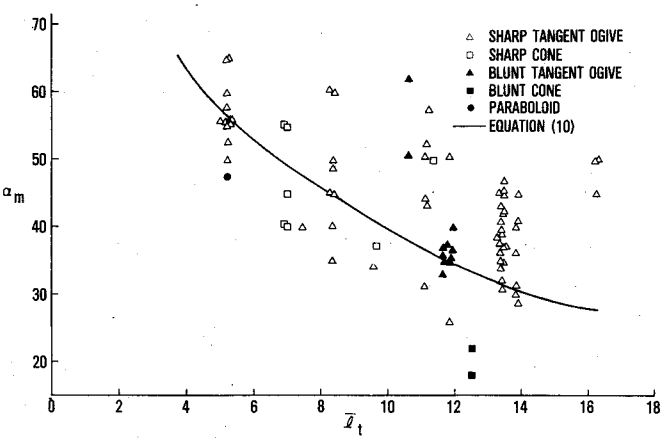

Fig. 8 α_m vs $\bar{\ell}_t$ for all points in the data base where α_m is known and $C_{ym}>0.75$.

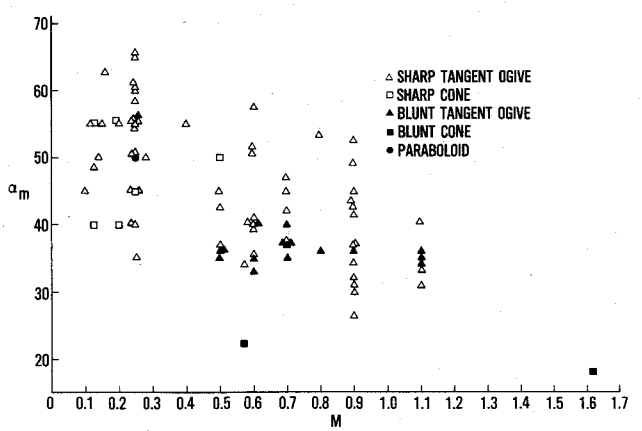

Fig. 9 α_m vs M for all points in the data base where α_m is known and $C_{ym}>0.75$. Solid line represents Eq. (10).

In all three figures only values of α_0 and α_m, corresponding to the case $C_{ym}>0.75$, are included. An excessive amount of scatter was found in the remaining points, a result of the difficulty in reading them.

Creation of a Predictive Model

The predictive equations are developed using Efroymson's multiple regression analysis technique.[15] Once a model has been postulated this method adds terms, one by one, to the regression equation, taking the factor with the highest correlation coefficient first. Before this variable is actually included in the model, an F test[16] is applied to its variance contribution, to determine whether it is statistically significant at a specified F level. At the end of each step, prior to the addition of a new variable, all variables in the model are checked to determine if they are statistically significant; those which are not, are dropped.

In order to determine successfully a predictive model using the above algorithm, the correct variables must be included in the proposed set. Although statistically insignificant variables are not incorporated, it is possible for incorrect terms to be in-

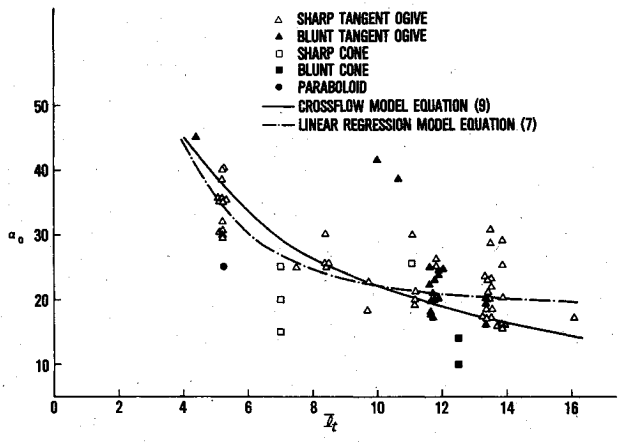

Fig. 10 α_0 vs $\bar{\ell}_t$ for all data points where α_0 is known and $C_{ym} > 0.75$. Also shown are Eqs. (7) and (8).

cluded as a result of peculiarities in the data base. Accordingly, in order to find a model which is physically reasonable, it is necessary to postulate an initial model which is as accurate as possible.

The modeling of C_{ym} is considered first, and the following predictive equation is proposed:

$$C_{ym} = b_0 + b_1 M + b_2 M^2 + \frac{b_3}{\ell_n} + \frac{b_4}{\ell_n^2} + b_5 \left(\frac{M}{\ell_n}\right) + b_6 f(Re,M) + b_7 r_b \tag{1}$$

Here, $f(Re,M)$ is defined as follows:

$$f(Re,M) = \begin{cases} 0 & M > 0.57 \text{ or } Re < 6(10^5) \\ 1 & M \leq 0.57 \text{ and } Re \geq 6(10^5) \end{cases}$$

This form for $f(Re,M)$ is suggested by a consideration of a cylinder in crossflow. Here, a sharp decrease in the side force or lift accompanies the transition of the boundary layer from laminar to turbulent conditions at subcritical Mach numbers.[13] The remaining terms are included on the basis of trends evident in the examination of the data base. The variable ℓ_n has been used in inverted form, to insure that in the limit $\ell_n \to \infty$, a finite force is obtained. For tangent ogive bodies to which this model will be applied, the smallest possible value of ℓ_n is 0.5, and the limit $\ell_n \to 0$ need not be considered.

Trends evident in the data establish that the type of body has a strong influence on side force. This suggests that a separate predictive equation should be developed for each class of body, a procedure which is practical in terms of the available data base only for sharp and blunt tangent ogives with constant diameter afterbodies. The proposed model defined in Eq. (1) is applied to both of these types of bodies, with b_7 set equal to zero for sharp tangent ogives. Requiring a 95% confidence level[16] for the entering or leaving of a particular variable results in the following predictive equations:

1) Sharp tangent ogives ($r_b < 0.005$)

$$C_{ym} = 4.20 - 12.50\, h\left(\frac{M}{\ell_n}\right) - 1.06\, f(Re,M) \tag{2a}$$

with a standard error of $C_{ym} = 0.65$ where

$$h\left(\frac{M}{\ell_n}\right) = \begin{cases} 0.3 \text{ for } \dfrac{M}{\ell_n} \geq 0.3 \\ \dfrac{M}{\ell_n} \text{ for } \dfrac{M}{\ell_n} < 0.3 \end{cases} \tag{2b}$$

2) Blunt tangent ogives ($r_b > 0.005$)

$$C_{ym} = 1.17 - 0.543\, f(Re,M) - 3.91 h'\left(\frac{M}{\ell_n}\right) \tag{3a}$$

with a standard error of $C_{ym} = 0.38$ where

$$h'\left(\frac{M}{\ell_n}\right) = \begin{cases} 0 & M \leq 0.57 \\ \dfrac{M - .57}{\ell_n} & M > 0.57 \end{cases} \tag{3b}$$

The special limits on M/ℓ_n described in functions h and h' are suggested by an examination of the residuals, rather than of physical characteristics.

As an alternative to Eq. (2a), a model is proposed using M_c and Re_c in place of M and Re. Here again the form of Eq. (1) is assumed with $b_7 = 0$ and $f(Re_c,M_c)$ defined as

$$f(Re_c,M_c) = \begin{cases} 0 & M_c > 0.5 \text{ or } Re_c \leq 4.25(10^6) \\ 1 & M_c \leq 0.5 \text{ and } Re_c > 4.25(10^6) \end{cases}$$

This yields

$$C_{ym} = 3.65 - 1.019\, M_c^2 - 8.39\, h\left(\frac{M_c}{\ell_n}\right) - 0.889\, f(Re_c,M_c) \tag{4}$$

with a standard error of $C_{ym} = 0.70$. Here, the function h is defined by Eq. (2b). Although this equation does not provide as good a fit as Eq. (2a), it can be used to generate an upper bound for $|C_y|$ as a function of α.

In interpreting results from Eqs. (2-4), negative values of C_{ym} indicate an expected side-force magnitude of zero.

Visible trends in the data base relate α_m to M and $\bar{\ell}_t$, which suggests the following model:

$$\alpha_m = b_0 + b_1 M + b_2 M^2 + \frac{b_3}{\bar{\ell}_t} + \frac{b_4}{\bar{\ell}_t^2} + b_5 \frac{M}{\bar{\ell}_t} \tag{5}$$

Here again, $\bar{\ell}_t$ is included in inverted form in order that finite results may be obtained in the limit $\bar{\ell}_t \to \infty$. The case $\bar{\ell}_t \to 0$ is not of practical interest. The final predictive equation is

$$\alpha_m = 39.8 - 10.3M + \frac{91.6}{\bar{\ell}_t} \tag{6}$$

with a standard error of $\alpha_m = 6.75$.

Only values of α_m corresponding to $C_{ym} > 0.75$ are represented in this equation, for the previously mentioned reasons; for cases having two identical C_{ym} peaks, both values of α_m are used.

The variable α_0 is indicated to be a function of $\bar{\ell}_t$, as shown in Fig. 10. A secondary relationship with M possibly exists, and a model of the form of Eq. (5) is assumed. This yields

$$\alpha_0 = 18.22 + 425.7/\bar{\ell}_t^2 \tag{7}$$

with a standard error of $\alpha_0 = 4.95$. Hence, the postulated relation between α_0 and M lacks sufficient statistical evidence to be included in the model.

Analysis of Regression Models

Peak values of C_y are strongly influenced by the nose geometry, while model length does not appear to be an important parameter. This suggests that maximum side forces are generated on the nose by the surrounding flowfield and are essentially a nose phenomenon.

The final regression equations indicate that on tangent ogives, C_{ym} is a weak function of Re, decreasing under the conditions of turbulent separation at subcritical Mach numbers. This relation should be considered as tentative, since most of the high Re points are from a single facility,[1] and the supposed Re influence possibly may be a facility effect.

The variable $\bar{\ell}_t$ plays a dominant role in determining α_m and α_0. A simple model can be constructed to explain this relationship using the impulsive flow analogy.[13] This analogy assumes that the crossflow plane is swept at the uniform rate $U\cos\alpha$ down the length of the body. The developing flow in the crossflow plane is analogous to a two-dimensional cylinder in impulsively started flow. Distance along the body x is related to time from the start of flow in the case of the cylinder by $x=U\cos(\alpha)t$. Experimental data for incompressible flow, covering the Re range $0.15(10^5)$ to $1.2(10^5)$, indicates that wake asymmetries first develop at[17] $t^*=Ut/D=4$. Applying this especially to a body at incidence, and using the impulsive flow analogy, yields

$$x\ \tan\alpha_0/\bar{D}=\bar{\ell}_t\ \tan\alpha_0=4 \tag{8}$$

Solving for α_0

$$\alpha_0=\tan^{-1}\left\{\frac{4}{\bar{\ell}_t}\right\} \tag{9}$$

Good agreement exists between this relation and the regression model of Eq. (7), as is shown in Fig. 10.

The experimental data of Ref. 17 also indicate that the first large vortex is shed at $t^*=8.5$. Using this in Eq. (8), and solving for α

$$\alpha=\tan^{-1}\left\{\frac{8.5}{\bar{\ell}_t}\right\} \tag{10}$$

This expression yields an α which falls within the range of values given by the data base, as is shown in Fig. 8. The implication is that peak side-force values are associated typically with the shedding of the first large vortex.

The dependence of α_m on M can be understood by noting that C_{ym} decreases with increasing M_c (see Fig. 4). Models tested in transonic or supersonic flow will experience large values of M_c, and small values of C_y, at high angles of attack. Hence, the maximum value of C_y will occur at lower incidences, where M_c is small and C_y is large.

Conclusions

Measurable side forces are obtained up to a Mach number of 1.4 on tangent ogives, and 2.0 on cones. The critical model dimension in determining peak side load is the nose fineness, which suggests that maximum side loads are associated with the flow about the model nose. Blunt tangent ogives show a lower level of side force than do sharp ones, but the degree of bluntness does not appear to be important. Good agreement between the regression model and the crossflow model indicates that side forces arise in a manner which is consistent with the predictions of the impulsive flow analogy. In addition, peak side forces occur at an angle of attack defined by the impulsive flow analogy to correspond approximately to the shedding of the first large vortex.

The linear regression equations for C_{ym}, x_0, and α_m developed in this report, provide a method of estimating values of these parameters. These specific equations, which should be updated when a more comprehensive data base becomes available, are a product and not a part of this paper's theme. The central idea is that realistic prediction methods for bodies at high angles of attack in the subsonic transonic range must take into account the sensitive nature of the flowfield. The load on, and the flowfield about such bodies will fluctuate for reasons which are difficult to identify and often not practical to control. Quantitative conclusions concerning the characteristics of side force cannot be drawn from a limited number of tests, but can only be determined statistically by considering a large number of measurements. A physical understanding of the phenomena is essential for the development of an optimum model.

References

[1] Keener, E. R. and Chapman, G. T., "Onset of Aerodynamic Side Forces at Zero Sideslip on Symmetric Forebodies at High Angles of Attack," AIAA Paper 74-770, Anaheim, Calif., 1974.

[2] Pick, G., "Investigation of Side Forces on Ogive-Cylinder Bodies at High Angles of Attack in the $M=0.5$ to 1.1 Range," AIAA Paper 71-570, Palo Alto, Calif., 1971.

[3] Fleeman, E. L. and Nelson, R. C., "Aerodynamic Forces and Moments on a Slender Body with a Jet Plume for Angles of Attack up to 180 Degrees," AIAA Paper 74-110, Washington, D.C., 1974.

[4] Clark, W. H., Peoples, J. R., and Briggs, N. M., "Occurrence and Inhibition of Large Yawing Moments During High Incidence Flight of Slender Missile Configurations," *Journal of Spacecraft*, Vol. 10, Aug. 1973, pp. 510-519.

[5] Coe, P. L. Jr., Chambers, J. R., and Letko, W., "Asymmetric Lateral-Directional Characteristics of Pointed Bodies of Revolution at High Angles of Attack," NASA TN D-7095, Nov. 1972.

[6] Gowen. F. C. and Perkins, E. W., "Study of the Effects of Body Shapes on the Vortex Wakes of Inclined Bodies at $M=2$," NACA RM A53117, 1963.

[7] Thomson, K. D. and Morrison, D. F., "The Spacing, Position and Strength of Vortices in the Wake of Slender Cylindrical Bodies at Large Incidence," *Journal of Fluid Mechanics*, Vol. 50, 1971, pp. 751-783.

[8] Smith, L. H. and Nunn, R. H., "Aerodynamic Characteristics of an Axisymmetric Body Undergoing a Uniform Pitching Motion," NPS-59 N 75021, Feb. 1975.

[9] Jorgensen, L. H. and Nelson, E. R., "Experimental Aerodynamics Characteristics for a Cylindrical Body of Revolution with Various Noses at Angles of Attack from 0 to 58° and Mach Numbers from .6 to 2.0," NASA TMX-3128, Dec. 1974.

[10] Jorgensen, L. H. and Nelson, E. R., "Experimental Aerodynamic Characteristics for Bodies of Elliptic Cross Section at Angles of Attack from 0 to 58° and Mach Numbers from .6 to 2.0," NASA TMX-3129, Feb. 1975.

[11] Daniels, P., "Minimization of Lock-In Roll Moment on Missiles Via Slots," NSWC/DL Tech. Rept. TR-3250, Jan. 1971.

[12] Wardlaw, A. B. Jr., "Prediction of Normal Force, Pitching Moment, and Yaw Force on Bodies of Revolution at Angles of Attack up to 50 Degrees Using a Concentrated Vortex Flow-Field Model," NOLTR 73-209, Oct. 1973.

[13] Wardlaw, A. B. Jr. and Morrison, A. M., "Induced Side Forces on Bodies of Revolution at High Angle of Attack," NSWC/WOL/TR 75-176, Dec. 1975.

[14] Orlik-Ruckerman, K. J., La Berge, J. G., and Iyengar, S., "Half and Full Model Experiments on Slender Cones at Angle of Attack," *Journal of Spacecraft and Rockets*, Vol. 11, Sept. 1973, pp. 575-580.

[15] Efroymson, M. A., "Multiple Regression Analysis," *Mathematics Methods for Digital Computers*, Ralston and Wilt, editors, J. Wiley, New York, 1962, pp. 191-203.

[16] Draper, N. R. and Smith, H., *Applied Regression Analysis*, J. Wiley, New York, 1966, pp. 24-26.

[17] Sarpkaya, T., "Separated Flow about Lifting Bodies and Impulsive Flow about Cylinders," *AIAA Journal*, Vol. 4, March 1966, pp. 414-420.